GEOPHYSICAL RESEARCH LETTERS, VOL. 37, L12705, doi:10.1029/2010GL043730, 2010

Temporary acceleration of the hydrological cycle in response to a CO_2 rampdown

Peili Wu,[1] Richard Wood,[1] Jeff Ridley,[1] and Jason Lowe[1]

Received 26 April 2010; revised 6 May 2010; accepted 17 May 2010; published 23 June 2010.

[1] Current studies of the impact of climate change mitigation options tend to scale patterns of precipitation change linearly with surface temperature. Using climate model simulations, we show a nonlinear hydrological response to transient global warming and a substantial side effect of climate mitigation. In an idealised representation of mitigation action, where we reverse the trend of global warming, the precipitation response shows significant hysteresis behaviour due to heat previously accumulated in the ocean. Stabilising or reducing CO_2 concentrations in the atmosphere is found temporarily to strengthen the global hydrological cycle, while reducing rainfall over some tropical and subtropical regions. The drying trend under global warming over The Amazon, Australia and western Africa may intensify for decades after CO_2 reductions. The inertia due to accumulated heat in the ocean implies a commitment to hydrological cycle changes long after stabilisation or reduction of atmospheric CO_2 concentration. **Citation:** Wu, P., R. Wood, J. Ridley, and J. Lowe (2010), Temporary acceleration of the hydrological cycle in response to a CO_2 rampdown, *Geophys. Res. Lett.*, *37*, L12705, doi:10.1029/2010GL043730.

1. Introduction

[2] The most direct impact of global warming comes from changes in the hydrological cycle (HC), affecting droughts, floods and water supplies. On annual or longer timescales, global precipitation P and evaporation E (including sublimation from snow and sea ice and surface evapotranspiration) must balance as the moisture holding capacity (water vapour content or WVC) of the atmosphere is small [*Trenberth*, 1998]. The WVC defines the size of the atmospheric "reservoir" whilst E and P define the cycling rate of water in and out of the reservoir (the HC).

[3] The WVC of the atmosphere closely follows the saturation vapour pressure as a near exponential function of temperature described by the Clausius-Clapeyron (CC) relation. At temperatures typical of the lower troposphere, it is predicted to increase by 7%/K [*Mitchell et al.*, 1987; *Allen and Ingram*, 2002; *Held and Soden*, 2006]. This has been verified by both models and observations [*Held and Soden*, 2006; *Wentz et al.*, 2007]. However, it has long been realised that changes in global HC differ significantly from changes in WVC [e.g., *Mitchell et al.*, 1987]. If one defines hydrological sensitivity as percentage change of global mean precipitation per degree surface warming, only 1–3%/K is predicted by climate models [*Cubasch et al.*, 2001; *Lambert and Webb*, 2008]. In other words, the size of the reservoir does not determine the flux in/out. Although it is generally expected that the HC will intensify with global warming, it is not absolutely clear why we expect that to happen. We know that, in equilibrium, increased latent heat release due to a stronger HC must be balanced by net radiative cooling from the atmosphere [*Allen and Ingram*, 2002]. During a transient climate simulation, increasing greenhouse gas (GHG) concentrations in the atmosphere will initially reduce precipitation due to lapse rate effect before significant warming of the surface takes place [*Mitchell et al.*, 1987; *Yang et al.*, 2003].

[4] The global HC is driven primarily by net radiative energy at the surface [*Wild et al.*, 2008; *Andrews et al.*, 2009], but constrained by atmospheric lapse rate or radiative cooling [*Allen and Ingram*, 2002; *Yang et al.*, 2003]. Net downward solar short wave (SW) R_{Snet} and atmospheric long wave (LW) radiation R_{LD} provide the total available energy to the Earth's surface, which is transmitted back to the atmosphere in the form of LW radiation R_{LU} (~80%), latent heat flux via evaporation Q_L (~16%), sensible heat flux via conduction and turbulent exchange Q_S (~3%) and a small amount taken up by the ocean G, to maintain a relatively stable modern climate [*Trenberth et al.*, 2009]. Perturbations to the energy supply will cause the system to readjust. The HC is expected to intensify along with increased atmospheric GHG concentrations as a warmer atmosphere emits more downward LW radiation, increasing net surface energy availability.

2. Hydrological Hysteresis

[5] Hydrological sensitivity is usually estimated from equilibrium climate simulations (e.g., $2xCO_2$) and regarded as constant [*Cubasch et al.*, 2001]. Following on from a constant hydrological sensitivity, climate mitigation studies [e.g., *Mitchell*, 2003; *Wilby et al.*, 2009] tend to assume a linear relationship between temperature and precipitation. In practice, there is a need to assess transient climate change and the impact of various mitigation actions in the near future. To investigate hydrological response to transient global warming and potential mitigation actions, a set of climate simulations are conducted using the standard HadCM3 model. The model is forced with a 2% annual increase in CO_2 from preindustrial values (280 ppm) until it reaches 4x (1120 ppm) after 70 years. Two climate trajectories are produced, the first (EXPT1) follows the period of increasing with an immediate decline in CO_2, at 2% a year, back to pre-industrial concentrations. The second simulation (EXPT2) stabilises CO_2 at 1120 ppm for 1270 years before declining at 2% per year. For both trajectories, the runs are continued for 150 yr after CO_2 returns to preindustrial values.

[1]Met Office Hadley Centre, Exeter, UK.

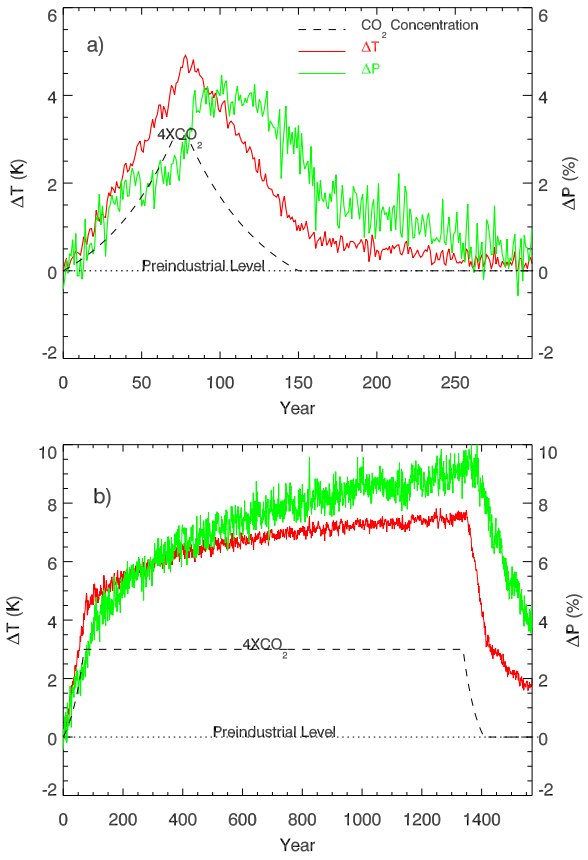

Figure 1. Time evolution of annual mean atmospheric CO_2 concentration (black dashed line), surface air temperature (red) and precipitation (green) anomalies relative to the control simulation for (a) EXPT1 and (b) EXPT2. The rate of CO_2 changes is 2% per year for both the rampup and rampdown periods.

Figure 1 shows the time evolution of CO_2, ΔT and ΔP for EXPT1 (Figure 1a) and EXPT2 (Figure 1b). The first parts of the two are identical so it is better to see Figure 1a. During this rampup phase, the rate of warming seems steady following the rise of CO_2; however, precipitation response is very different. The rate of precipitation increase slows down significantly after CO_2 doubling. The most interesting signal from Figure 1a is the precipitation response to a CO_2 reduction. Temperature falls immediately following the rampdown of CO_2, but, instead of falling, precipitation jumps up dramatically to a new level and maintains the high level for several decades before starting to fall. It takes 150 years for the global HC to return to the preindustrial level, long after CO_2 returns. If we stabilize at the 4x level, global warming and the HC intensification continue beyond the 1270 yr simulation (Figure 1b). Although the warming rate slows down after the first few hundred years, the intensification of the HC does not slow down. Warming increases by a further 3.5K during the stabilization phase, while the HC strengthens by a further 5.5%. Comparing to a 4K warming and 4% increase in precipitation during the rampup phase, hydrological sensitivity is stronger during the stabilization period (1%/K versus 1.6%/K). These measures clearly suggest that hydrological sensitivity is not constant during transient climate change and hydrological response is more complicated than temperature response.

[6] In order to see hydrological sensitivities during different phases of the experiments, we have plotted ΔP against ΔT for both experiments and the entire periods (Figures 2b and 2d). To illustrate the fundamental difference between WVC response and response of the HC, scatter plots of ΔWVC against ΔT are also included (Figures 2a and 2c). It is very clear that WVC is a simple monotonic function of temperature and it is completely reversible. This just confirms previous conclusions [e.g., *Mitchell et al.*, 1987] that the moisture holding capacity (or the size of the reservoir) of the atmosphere is controlled by temperature and follows the CC relationship. The HC is also a function of temperature, but it is not only of function of temperature. Varying CO_2 in the atmosphere leads to a hysteresis of the HC. From Figure 2, it is clear that the HC follows different paths during the rampup and rampdown phases of atmospheric CO_2. At a given surface warming, there are two possible hydrological states. Here the external forcing comes from input of CO_2 and the system memory is likely to come from the oceans as we will see in the following section. Reducing CO_2 from a raised concentration level (with or without stabilization) leads to a temporary strengthening of the global HC. This would be a significant side effect of climate mitigation or geoengineering using a CO_2 removal option. As geoengineering options, both reducing CO_2 and reducing solar radiation can reduce global warming, but the hydrological responses are opposite. Reducing solar radiation leads to a weakening [*Bala et al.*, 2008] while reducing CO_2 leads to a temporary strengthening of the global HC.

[7] Note that the relationship between precipitation and temperature is not linear under varying GHG forcing due to the competing effects of surface warming and suppression of LW cooling [*Yang et al.*, 2003]. With a *fixed* level of GHGs (1x or 4xCO_2), the P~T relationship is linear as shown by the blue stars in Figures 2b and 2d. This is also the case when comparing equilibrium double-CO_2 responses from a range of slab models [*Allen and Ingram*, 2002]. Hydrological sensitivity to temperature is clearly larger when GHG concentrations are constant than when they are varying. This behaviour is also observed in other IPCC AR4 models (not shown here). This is because the direct influence of GHG on P is negative, which has been described as the temperature independent radiation term in atmospheric energy budget [*Allen and Ingram*, 2002] or the fast response term in a surface energy budget framework [*Andrews et al.*, 2009]. When GHG concentration is fixed, this term is a constant determined by the intercepts in a P~T diagram, where one finds a linear P~T relationship. The level of this negative impact does not depend on temperature, but depends on GHG concentration. As GHG concentration varies, we see a nonlinear P~T relationship because both factors now affect precipitation.

3. Mechanism

[8] To understand the controlling mechanism for the hydrological hysteresis, we examine the global mean surface energy budget:

$$R_{Lnet} + R_{Snet} = Q_L + Q_S + G \quad (1)$$

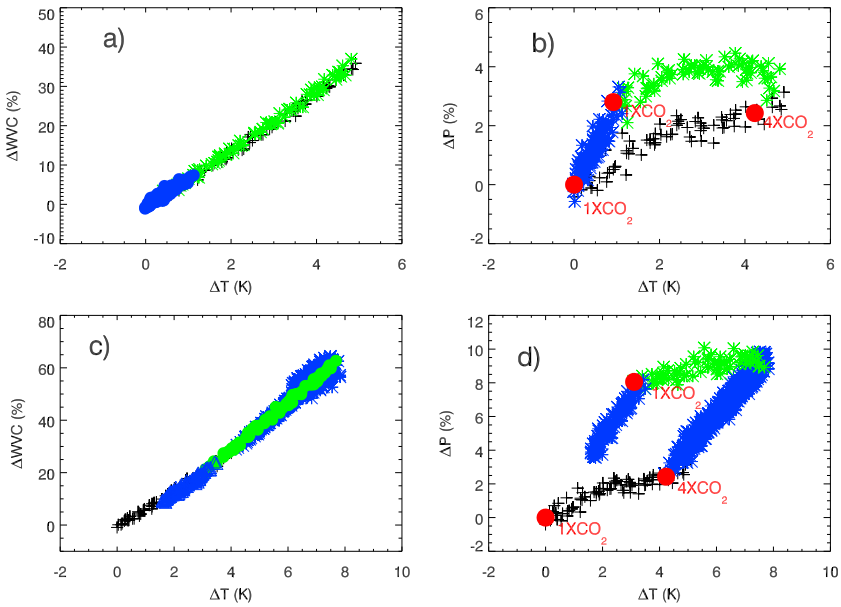

Figure 2. Scatter plots of (a, c) WVC changes and (b, d) precipitation changes against surface temperature changes in two sets of experiments using the standard HadCM3 model showing the reversibility of WVC changes (Figures 2a and 2c) and hysteresis of the global hydrological cycle (Figures 2b and 2d). Black colour shows the rampup simulation, green the rampdown and blue the stabilisation runs. The red spots mark the CO_2 concentrations.

where $R_{Lnet} = R_{LD} - R_{LU;}$ R_{LD} and R_{LU} are downward and upward LW radiation, $R_{Snet} = R_{SD} - R_{SU;}$ R_{SD} and R_{SU} are downward and upward SW radiation. Latent heat flux Q_L can be expressed as either LE or LP, where L is the latent heat constant, Q_S is sensible heat flux. As the heat capacity of the atmosphere is negligible, ocean heat uptake (OHT) G must be balanced by net radiation at the top of the atmosphere $G = -R_{TOA}$ (R_{TOA} positive upwards), assuming land heat uptake is negligible. The perturbation energy budget equation is then

$$L\Delta P = \Delta R_{Lnet} + \Delta R_{Snet} - \Delta Q_S + \Delta R_{TOA} \quad (2)$$

[9] Equation (2) states that the hydrological response depends on the net surface energy availability: ΔR_{Lnet} shows the GHG contributions, water vapour, lapse rate and LW cloud feedbacks, ΔR_{Snet} are the SW cloud, surface albedo feedbacks and atmospheric absorption of solar radiation (ASR), ΔQ_S changes in the Bowen ratio [*Held and Soden*, 2006] and ΔR_{TOA} system adjustment (OHT). In equilibrium, $\Delta R_{TOA} = 0$, equation (2) represents the conventional tropospheric energy balance considered by previous studies [*Mitchell et al.*, 1987; *Allen and Ingram*, 2002]. Our approach is consistent with the previous tropospheric energy budget theories [cf. *Allen and Ingram*, 2002, equation (1)], but while these theories consider atmospheric LW radiative cooling as a controller to precipitation our surface budget theory identifies the climate drivers of surface evaporation.

[10] The advantage of using (2) is to provide insight into the physical processes that drive the global HC under transient climate change. Increasing anthropogenic GHG concentrations lead to a positive contribution to ΔR_{Lnet} and warming induced WVC increase adds more positive feedbacks to this term. This is where the link between WVC and the HC exists; the rate of precipitation change is influenced via the extra radiative energy supplied by the increased WVC. As ΔR_{Lnet} is dominated by water vapour feedbacks that are strongly constrained by the CC relation, the spread among different climate models should be small. The sign of ΔR_{Snet} is uncertain: melting of snow and sea ice leads to a positive contribution due to a reduction in surface albedo; cloud SW feedbacks are likely to be positive as most models predict less cloud in a warmer climate [*Trenberth and Fasullo*, 2009]; but increasing ASR due to increased WVC makes a negative contribution. Large uncertainties associated with cloud simulation are most likely responsible for the large spread in hydrological projections within contemporary climate models. Global changes in surface sensible heat flux ΔQ_S are of uncertain sign due to uncertainties in model simulations of the land-sea contrast, but will be seen to be small. Over the oceans, there is a marked reduction of sensible heat flux due to decreased air-sea temperature difference as GHG warms the atmosphere more than the oceans [*Lu and Cai*, 2009]. The opposite signs of change between sensible and latent heat fluxes over the oceans under GHG forcing lead to a reduction in the Bowen ratio. While GHGs are increasing, OHT or $-\Delta R_{TOA}$ is the only term definitively to slow down the intensification of the HC.

[11] Figure 3 shows the terms in equation (2) for EXPT1. It shows $L\Delta P$ (thick solid black line) in comparison to the sum of all the terms on the rhs (dashed line). The small discrepancies are due to the omission of atmospheric heat content changes. The dominant term in the perturbed global mean surface energy budget is net downward LW radiation. It closely follows atmospheric CO_2 concentrations and surface temperature, peaking at year 80. However its increase and decrease are almost symmetrical, and therefore, cannot explain the hysteresis behaviour in latent heat flux. The contribution from sensible heat flux is small. Changes

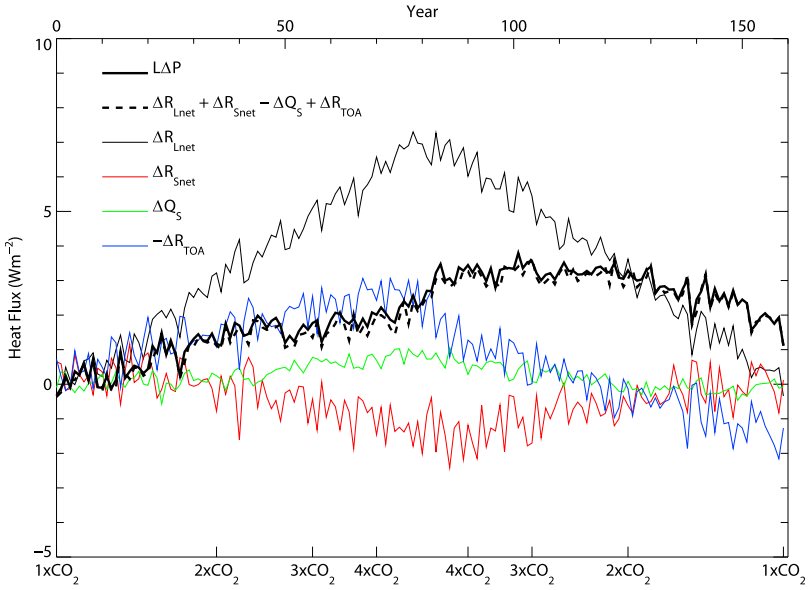

Figure 3. The perturbation surface energy budget for EXPT1, in which the CO_2 ramps down immediately following a rampup to 4x CO_2. It shows that the main surface energy driver for the hydrological hysteresis is ocean heat uptake.

in SW radiation make a moderate negative contribution. For low CO_2 levels, influence from SW radiation is negligibly small [see also *Lambert and Webb*, 2008]. SW influence increases towards higher CO_2 concentrations due to water vapour absorption [*Trenberth and Fasullo*, 2009]. OHT appears to be the process responsible for the hysteresis. During the rampup phase, OHT increases at a similar rate to latent heat flux until CO_2 peaks. As soon as CO_2 starts to decline, OHT declines rapidly while net downward LW radiation remains near its peak values, allowing more surface energy to be used for latent heat flux. OHT reverses sign in less than 40 years. As OHT equals TOA radiation imbalance, the driving process of the hydrological hysteresis can also be understood in terms of outgoing LW radiation. Reducing GHG concentrations allows more LW radiation to escape; increasing the atmosphere's cooling capacity and consequently precipitation.

4. Discussion

[12] In both EXPT1 and EXPT2, the strength of the global mean HC remains much stronger than the initial states after CO_2 levels are brought back to the starting point (1xCO_2). The difference is 2.48% for EXPT1 and 7.52% for EXPT2. In fact, regional changes are much greater than the global means. Figure 4 shows the difference of mean precipitation between the first decade of the rampup experiment and the last decade of the rampdown simulation after the long stabilisation phase (EXPT2). The two model states are marked by the two 1xCO_2 red spots in Figure 2d. CO_2 concentrations

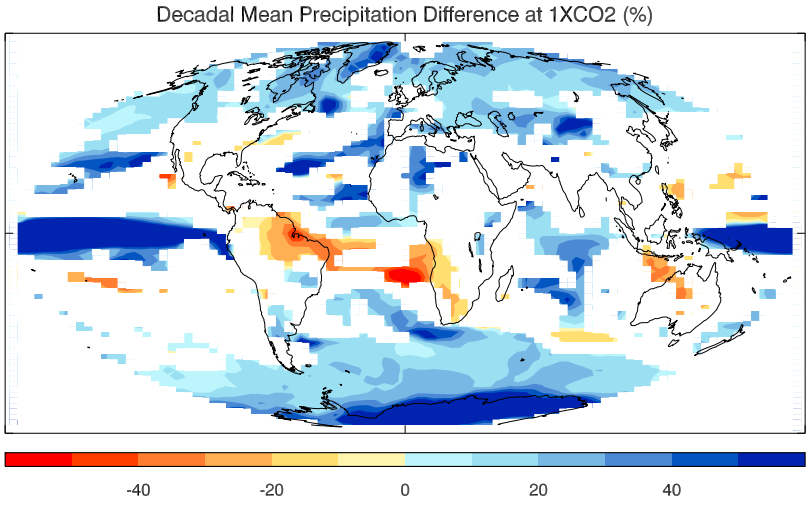

Figure 4. Geographic distributions of decadal mean precipitation differences after CO_2 returns to the preindustrial level for EXPT2: blue shows percentage increase in mean precipitation relative to the control simulation and red shows decrease. Statistically insignificant changes have been masked out at the 90% level assuming normal distribution.

in both periods are the same, but precipitation in most parts of world is very different. Although the overall HC is 7.52% stronger, precipitation does not increase everywhere. The high-latitudes of both hemispheres are considerably wetter, while in the tropics and subtropics, many areas are considerably drier. The most striking feature for regional changes is an over 50% reduction of annual mean precipitation across the southern Tropical Atlantic Sector from the Amazon to South Africa. The maritime continent and Australia are also noticeably drier. In some of these regions such as the Amazon, Australia and western Africa this means that the drying trend under global warming [*Cubasch et al.*, 2001; *Meehl et al.*, 2007] may continue to intensify for decades after CO_2 reductions. On the other hand, the increasing trend of precipitation over the high latitudes under global warming [*Wu et al.*, 2005, 2008] would also continue under falling CO_2 concentrations. Detailed mechanisms of regional HC response obviously demand further investigation. The leading pattern in the Tropical Atlantic Sector is believed to be associated with an overshoot response of the Atlantic meridional overturning circulation that is to be reported in a separate paper.

[13] The hysteresis behaviour of the global HC raises important implications associated with emission reduction or carbon capture from the atmosphere [*The Royal Society*, 2009]. Our results show that even if GHG concentrations are stabilised or reduced, the global HC is expected to continue to strengthen for decades to centuries. This effect must be taken into account when assessing the implications of various mitigation options for flooding, water supply, food production and human health. Pattern-scaling approaches that link regional precipitation to global temperature are often used to assess mitigation options [*Mitchell*, 2003; *Wilby et al.*, 2009], using relationships developed from scenarios of increasing GHG forcing. Our results suggest that such relationships between precipitation and warming may significantly underestimate precipitation changes during periods of stabilisation or reduction. The inertia due to the accumulated heat in the ocean implies a commitment to HC changes long after stabilisation.

[14] **Acknowledgments.** This work was supported by the Joint DECC, Defra and MoD Integrated Climate Programme—DECC/Defra (GA01101).

References

Allen, M. R., and W. J. Ingram (2002), Constraints on the future changes in the hydrological cycle, *Nature*, *419*, 224–232, doi:10.1038/nature01092.

Andrews, T., P. M. Forster, and J. M. Gregory (2009), A surface energy perspective on climate change, *J. Clim.*, *22*, 2557–2570, doi:10.1175/2008JCLI2759.1.

Bala, G., P. B. Duffy, and K. E. Taylor (2008), Impact of geoengineering schemes on the global hydrological cycle, *Proc. Natl. Acad. Sci. U. S. A.*, *105*, 7664–7669, doi:10.1073/pnas.0711648105.

Cubasch, U., et al. (2001), Projections of future climate change, in *Climate Change 2001: The Science of Climate Change. Contribution of Working Group I to the Third Assessment Report of the Intergovernmental Panel on Climate Change*, edited by J. T. Houghton et al., chap. 9, pp. 527–582, Cambridge Univ. Press, Cambridge, U. K.

Held, I. M., and B. J. Soden (2006), Robust responses of the hydrological cycle to global warming, *J. Clim.*, *19*, 5686–5699, doi:10.1175/JCLI3990.1.

Lambert, F. H., and M. J. Webb (2008), Dependency of global mean precipitation on surface temperature, *Geophys. Res. Lett.*, *35*, L16706, doi:10.1029/2008GL034838.

Lu, J., and M. Cai (2009), Stabilization of the atmospheric boundary layer and the muted global hydrological cycle response to global warming, *J. Hydrometeorol.*, *10*, 347–352, doi:10.1175/2008JHM1058.1.

Meehl, G. A., et al. (2007), Global climate projections, in *Climate Change 2007, The Physical Science Basis. Contribution of Working Group I to the Fourth Assessment Report of the Intergovernmental Panel on Climate Change*, edited by S. Solomon et al., chap. 10, pp. 747–845, Cambridge Univ. Press, Cambridge, U. K.

Mitchell, T. D. (2003), Pattern scaling, an examination of the accuracy of the technique for describing future climates, *Clim. Change*, *60*, 217–242, doi:10.1023/A:1026035305597.

Mitchell, J. F. B., C. A. Wilson, and W. M. Cunnington (1987), On CO_2 climate sensitivity and model dependence of results, *Q. J. R. Meteorol. Soc.*, *113*, 293–322, doi:10.1256/smsqj.47516.

The Royal Society (2009), Geoengineering the climate: Science, governance and uncertainty, report, London.

Trenberth, K. E. (1998), Atmospheric moisture residence times and cycling: Implications for rainfall rates with climate change, *Clim. Change*, *39*, 667–694, doi:10.1023/A:1005319109110.

Trenberth, J. E., and J. T. Fasullo (2009), Global warming due to increasing absorbed solar radiation, *Geophys. Res. Lett.*, *36*, L07706, doi:10.1029/2009GL037527.

Trenberth, J. E., J. T. Fasullo, and J. Kiehl (2009), Earth's global energy budget, *Bull. Am. Meteorol. Soc.*, *90*, 311–323, doi:10.1175/2008BAMS2634.1.

Wentz, F. J., L. Ricciardulli, K. Hilburn, and C. Mears (2007), How much more rain will global warming bring?, *Science*, *317*, 233–235, doi:10.1126/science.1140746.

Wilby, R. L., et al. (2009), A review of climate risk information for adaptation and development planning, *Int. J. Climatol.*, *29*, 1193–1215, doi:10.1002/joc.1839.

Wild, M., J. Grieser, and C. Schar (2008), Combined surface solar brightening and increasing greenhouse effect support recent intensification of the global land-based hydrological cycle, *Geophys. Res. Lett.*, *35*, L17706, doi:10.1029/2008GL034842.

Wu, P., R. Wood, and P. Stott (2005), Human influence on increasing Arctic river discharges, *Geophys. Res. Lett.*, *32*, L02703, doi:10.1029/2004GL021570.

Wu, P., H. Haak, R. Wood, J. Jungclaus, and T. Furevik (2008), Simulating the terms in the Arctic hydrological budget, in *Arctic-Subarctic Ocean Fluxes: Defining the Role of the Northern Seas in Climate*, edited by R. R. Dickson, J. Meincke, and P. Rhines, pp. 363–384, Springer, Dordrecht, Netherlands.

Yang, F., A. Kumar, M. E. Schlesinger, and W. Wang (2003), Intensity of hydrological cycles in warmer climates, *J. Clim.*, *16*, 2419–2423, doi:10.1175/2779.1.

J. Lowe, J. Ridley, R. Wood, and P. Wu, Met Office Hadley Centre, FitzRoy Road, Exeter EX1 3PB, UK. (peili.wu@metoffice.gov.uk)